

Machine Learning H -theorem

Ruben Lier^{1,2,3,*}

¹*Institute for Theoretical Physics, University of Amsterdam, 1090 GL Amsterdam, The Netherlands*

²*Dutch Institute for Emergent Phenomena (DIEP),
University of Amsterdam, 1090 GL Amsterdam, The Netherlands*

³*Institute for Advanced Study, University of Amsterdam,
Oude Turfmarkt 147, 1012 GC Amsterdam, The Netherlands*

H -theorem provides a microscopic foundation of the Second Law of Thermodynamics and is therefore essential to establishing statistical physics, but at the same time, H -theorem has been subject to controversy that in part persists till this day. To better understand H -theorem and its relation to the arrow of time, we study the equilibration of randomly oriented and positioned hard disks with periodic boundary conditions. Using a model based on the *DeepSets* architecture, which imposes permutation invariance of the particle labels, we train a model to capture the irreversibility of the H -functional.

CONTENTS

I. Introduction	1
II. Boltzmann equation	2
III. Hard disk simulation	2
IV. Machine learning H -theorem	3
V. Comparison with H -functional	4
VI. Discussion	5
VII. Methods	6
VIII. Acknowledgements	6
References	6

I. INTRODUCTION

The discovery of H -theorem by Ludwig Boltzmann in 1872 [1] played a pivotal role in establishing statistical mechanics as a framework that provides thermodynamics with a microscopic origin and liberates it from its axiomatic foundations. At the same time, H -theorem was for a long time the topic of much debate [2–4], parts of which persist to this day [5–8]. One lingering issue is the *Loschmidt paradox* [9, 10], which relates to the remarkable feature of H -theorem that there exists an H -functional which can only decrease in time and therefore signal the presence of an *arrow of time* [11] despite the system being *microscopically reversible* [12], which means that the particles of which the gas is composed undergo interactions that are time-reversal invariant. This paradox is now better understood, in part because of the discovery of BBGKY hierarchy [13, 14], which must be trun-

cated by assuming molecular chaos so that one is left with the Boltzmann equation. The assumption of molecular chaos introduces an arrow of time; while Lanford’s theorem [15–17] proves its validity in the Boltzmann–Grad limit [13] for short times, no general proof exists for arbitrary times or interaction types, so its adoption remains, to some extent, a leap of faith. Nevertheless, the Boltzmann equation has been found to be a valuable tool for deriving continuum equations from first principles that has been very widely used for more than a century [10, 18] in fields ranging from solid state physics [19–21] to high energy physics [22–24] as well as in active matter [25–28]. In recent years, several works tried to exploit the emergence of an arrow of time for many-particle systems as a way to better understand sequential data. For example, in Ref. [29], the authors show that by putting trajectories and their time-reverses into a binary classifier, it is possible to extract Crooks fluctuation theorem [30, 31] from the predicted probability of the binary classifier. In Ref. [32], the authors use siamese neural network to compare pairs of image sets at different times for a molecular dynamics simulation which involves a moving piston, enabling the authors to construct an entropy. This equilibrium entropy is shown to be consistent with thermodynamic axioms formulated by Lieb and Yngvason [33] and identical to the entropy of the van der Waals gas up to an affine transformation. Similarly, in Ref. [34], videos played forward and reversed are classified, and the classifier is then used to identify the spatial region in the video that has the strongest arrow of time. Lastly in Ref. [35], the authors learn a linear function that separates states early and late in time for games that have an irreversible element in it and therefore require safe exploration [36, 37]. The authors show that when such a function is learned for a two-component stochastic process the function has quantitative overlap with entropy up to an affine transformation. In this work, we learn to output a value that resembles H -functional up to an affine transformation for sequential data of a numerical simulation of randomly initialized hard disks [38–41]. We infer the H -functional using an approach that is similar to that of Ref. [35] where a linear

* r.liet@uva.nl

function is derived whose cost function is such that the learning processes pushes the model to learn to attribute higher output values to input values corresponding to later times.

The structure of this work is as follows. In Sec. II, we discuss Boltzmann equation and the related H -theorem. In Sec. III, we discuss the simulation performed to generate the data for which we wish to learn H -theorem, which is randomly initialized hard disks. In Sec. IV, we discuss the learning of H -theorem using a model that adheres to permutation invariance of the particle labels using the DeepSets architecture and learns a function that approaches H -theorem by requiring that it gives a higher value to input at later times.

II. BOLTZMANN EQUATION

We consider the number of particles dN in a region in phase space to be given by

$$dN = f(\mathbf{r}, \mathbf{v}, t) d\mathbf{r} d\mathbf{v} \quad , \quad (1)$$

where \mathbf{r} is the particle position, \mathbf{v} is its velocity and $f(\mathbf{r}, \mathbf{v}, t)$ is the distribution function. In the presence of a force \mathbf{F} , the Boltzmann equation is given by

$$\frac{\partial f}{\partial t} + \mathbf{v} \cdot \frac{\partial f}{\partial \mathbf{r}} + \frac{\mathbf{F}}{m} \cdot \frac{\partial f}{\partial \mathbf{v}} = \left(\frac{\partial f}{\partial t} \right)_{\text{self}} \quad , \quad (2)$$

where m is the particle mass. In this work, we set $\mathbf{F} = 0$ since the interactions are exclusively of the hard-sphere kind, and we also do not account for spatial dependence. The term in the right hand side of (2) is the collision integral for which one can find closure with the molecular chaos assumption [10, 42]. For the case of hard disks, the collision integral is given by [10, 18]

$$\left(\frac{\partial f}{\partial t} \right)_{\text{self}} = \iint d\mathbf{v}_2 db u (f(\mathbf{v}'_1, t) f(\mathbf{v}'_2, t) - f(\mathbf{v}, t) f(\mathbf{v}_2, t)) \quad , \quad (3)$$

where b is the impact parameter and \mathbf{v}'_1 and \mathbf{v}'_2 are velocities of particles going into the collision which are tied to \mathbf{v} and \mathbf{v}_2 through energy and momentum balance. Galilean invariance makes it that only the relative velocities $\mathbf{u} = \mathbf{v} - \mathbf{v}_2$ and $\mathbf{u}' = \mathbf{v}'_1 - \mathbf{v}'_2$ describe a unique collision, and the scattering angle χ that gives the relative angles between these two vectors is given by (see Fig. 1)

$$b = d \cos(\chi/2) \quad , \quad (4)$$

where d is the disk diameter. To solve (2) analytically for the exact collision operator is incredibly difficult. One way to do so is perturbatively, using the Chapman-Enskog expansion [18]. There exist however numerical approaches to solving (2) [43] and recently it has been

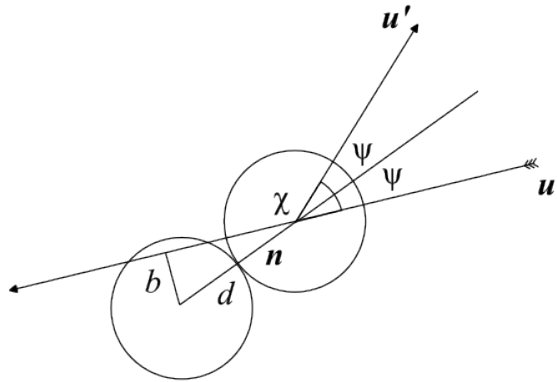


FIG. 1: Depiction of an elastic collision between two hard disks.

explored whether a neural network can be used to deal with the collision integral [44, 45]. Analytical challenges notwithstanding, H -theorem provides us with an excellent handle for understanding how (2) irreversibly moves towards an equilibrium state. To wit, H -theorem tells us that there exists an H -functional given by

$$H(t) = \int d\mathbf{v} f(\mathbf{v}, t) \log(f(\mathbf{v}, t)) \quad , \quad (5)$$

for which it holds that upon plugging in (2), one obtains

$$\frac{\partial}{\partial t} H(t) \leq 0 \quad . \quad (6a)$$

Furthermore, in two dimensions the equilibrium state is characterized by

$$\frac{\partial}{\partial t} H_0(t) = 0 \quad , \quad f_0(\mathbf{v}, t) = \frac{nm}{2\pi k_b T} \exp\left(-\frac{m}{2k_b T} |\mathbf{v} - \mathbf{v}_0|^2\right) \quad , \quad (6b)$$

where n is the particle density, T is temperature and \mathbf{v}_0 is the average velocity. $f_0(\mathbf{v}, t)$ is called the Maxwell-Boltzmann distribution. The striking elegance of (6) which emerges from the chaotic nature of hard disk collisions tells us that something very simple can be learned from very chaotic data and thereby underpins our machine learning approach.

III. HARD DISK SIMULATION

Let us now specify the simulation. The simulation is based on code from [46] and is initialized with 1000 hard disks of equal mass and diameter with random orientation and position in a square box with periodic boundary conditions. The initial velocity magnitude is chosen to be uniform, as a uniformly distributed velocity magnitude gives rise to an H -functional that undergoes only very

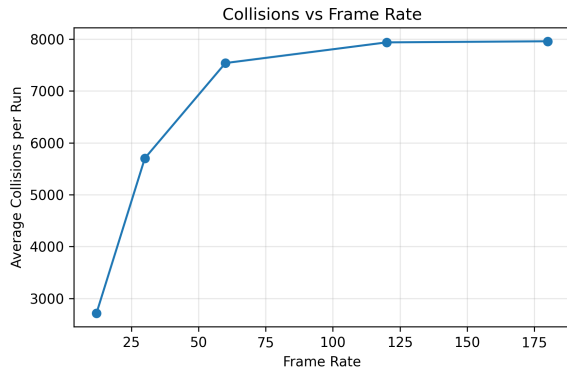


FIG. 2: Number of collisions that are observed in a single run averaged over 5 runs vs the frame rate. The frame rate is the inverse of the time step dt of the simulation.

minor changes through time and therefore it is not easy to see the downward trend dictated by H -theorem. For every timestep, it is checked whether two particles overlap, in which case an elastic collision takes place. This collision is constrained by energy and momentum balance and the requirement that momentum is only transferred in the direction parallel to the line of disk centers (see Fig. 1). Since all particles have the same mass, these collision rules can be described in terms of the simple relations

$$\mathbf{n} \cdot \mathbf{u}' = -\mathbf{n} \cdot \mathbf{u} \quad , \quad \mathbf{z} \times \mathbf{n} \times \mathbf{u}' = \mathbf{z} \times \mathbf{n} \times \mathbf{u} \quad , \quad (7)$$

where \mathbf{n} is the line of disk centers and \mathbf{z} is the out of plane direction. This collision only takes place if the relative velocity points oppositely to the line of disk centers, i.e. when it holds that

$$\mathbf{u} \cdot \mathbf{n} < 0 \quad . \quad (8)$$

as otherwise the particles are moving away from each other. If this constraint is not imposed, particles will get stuck together. The diameter of the disks is taken to be $d = 6 \cdot 10^{-3}$ whereas the periodic box has a unit surface. When the frame rate is too small, it is possible that certain collisions are missed. In Fig. 2, we show that at a frame rate of around 60, the number of collisions starts to plateau, so this is the frame rate we take. All velocities are saved for each timestep giving rise to an amount of $N_t = 500$ time steps, and we considered $N_{\text{run}} = 500$ unique runs. In Fig. 3, we show the distribution of the hard disks and compare it to the Maxwell-Boltzmann distribution of (6b).

IV. MACHINE LEARNING H -THEOREM

Let us now describe the machine learning process. At every training step, we have as input sequential data $\mathbf{V}_t^{[n]}$

for all t and n , where t corresponds to the time step and n corresponds to the run. For any run n , we have

$$\mathbf{v}_t^{(i),[n]} \in \mathbf{V}_t^{[n]} \quad , \quad (9)$$

where $\mathbf{v}_t^{(i),[n]}$ is the two-dimensional velocity vector of the i th particle. In order to effectively learn the H -functional, we utilize the permutation invariants of the particle labels, which is done with the DeepSets architecture [47]. In particular, we take the model to be of the form

$$h\left(\mathbf{V}_t^{[n]}\right) = \rho\left(\sum_i \phi\left(\mathbf{v}_t^{(i),[n]}\right)\right) \quad , \quad (10a)$$

where ρ and ϕ encode a neural network with trainable weights that treats any value of run n , any run t and any particle i on equal footing. Following [35], we consider a loss function per timestep $t \leq N_t - 1$ and run n that is given by

$$\begin{aligned} \mathcal{L}^{(0)}\left(\mathbf{V}_t^{[n]}, \mathbf{V}_{t+1}^{[n]}\right) &= h\left(\mathbf{V}_t^{[n]}\right) - h\left(\mathbf{V}_{t+1}^{[n]}\right) \\ &+ \lambda\left(h\left(\mathbf{V}_{t+1}^{[n]}\right) - h\left(\mathbf{V}_t^{[n]}\right)\right)^2 \end{aligned} \quad (10b)$$

The loss of (10b) contains a term that pushes to learn a function consistent with the monotonicity property (6a) as well as the term with coefficient λ that serves as a regularization. In Fig. 4, we give a graphical representation of the learning system of (10) and we see that the pairwise comparative nature of (10b) makes it so that this learning system effectively turns into a siamese neural network [48, 49]. After experimenting with (10), it is found that the trained function $h(\mathbf{V}_t)$, unlike the real H -functional, displays strongly oscillatory behavior upon increasing the time step. To mitigate this, we note that (6a) is an inequality which only requires that the H -functional does not increase as a function of time, not that it decreases. Therefore, we consider a generalization of the loss function of (10b) which is given by

$$\begin{aligned} \mathcal{L}^\alpha\left(\mathbf{V}_t^{[n]}, \mathbf{V}_{t+1}^{[n]}\right) &= \text{leaky-ReLU}\left(h\left(\mathbf{V}_t^{[n]}\right) - h\left(\mathbf{V}_{t+1}^{[n]}\right), \alpha\right) \\ &+ \lambda\left(h\left(\mathbf{V}_{t+1}^{[n]}\right) - h\left(\mathbf{V}_t^{[n]}\right)\right)^2 \quad . \end{aligned} \quad (11)$$

It follows that when $0 \leq \alpha < 1$, (11) makes sure that the function $h(\mathbf{V}_t)$ is punished more for incorrectly outputting a lower value at a later time step than it is rewarded for correctly outputting a higher value at later times. This choice is not only consistent with (6a), which only imposes the former on the H -functional, but also turns out to reduce oscillation of $h(\mathbf{V}_{t+1})$. We optimize for a total number of epochs $N_e = 120$ with the loss of (11) averaged over runs n and time steps t using the Adam optimizer [50], choosing learning rate $4 \cdot 10^{-4}$ and $\lambda = 0.2$. All the hidden layers of the model have hidden

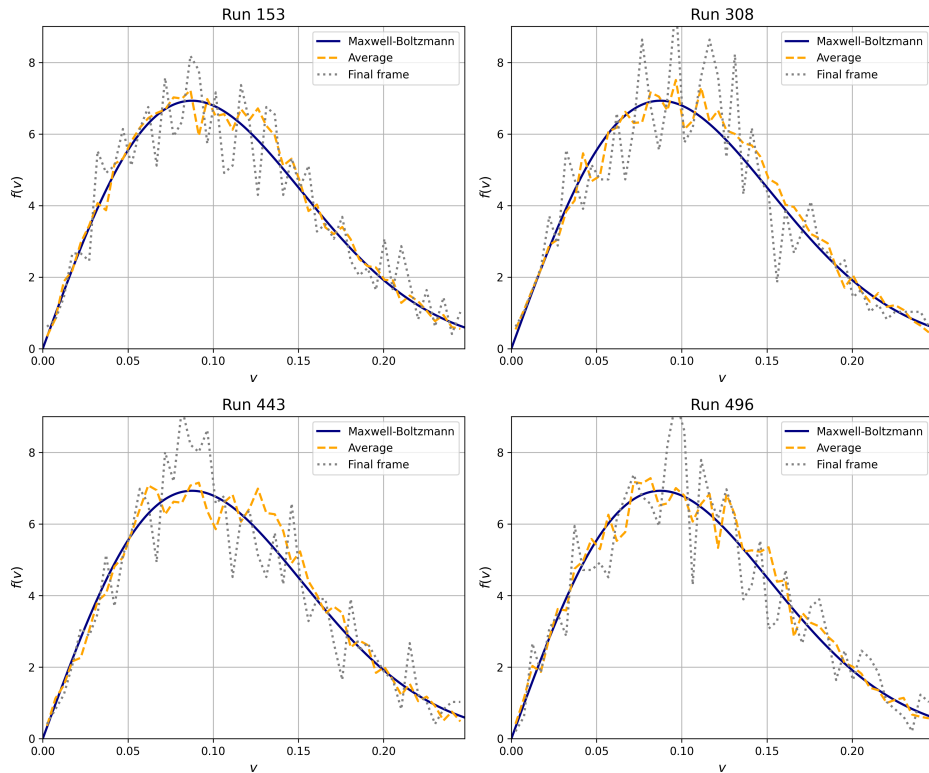


FIG. 3: Picture of theoretically predicted Maxwell-Boltzmann distribution together with average and final frame of hard disk simulation for the four different runs that are also considered in Fig. 5. For constructing the histograms, we used bin size 0.005. The uniform velocity magnitude at which the disks are initialized is given by $v = 0.12$, which means the Maxwell-Boltzmann distribution whose expression is given by (6b) has temperature $k_b T = 0.0076$ and mass $m = 1$. The averaging started after 20% of the run was completed.

dimension n_{hidden} and ReLU-activations (see Fig. 4 and Table I). While training, we increase α as a function of epoch e as

$$\alpha(e) = 1 - \frac{1 - \alpha_{\text{final}}}{N_e} \cdot e . \quad (12)$$

We train three distinct models with hidden dimensions

$$n_{\text{hidden}} \in \{16, 32, 64\} . \quad (13)$$

Because of the choice of a gradual increase according to (12) with a high α_{final} , one eventually reaches a point for all of the models where $\mathcal{L}_t^{\alpha(e)} > 0$, which indicates that the trivial solution where $h(\mathbf{V}_{t+1}) - h(\mathbf{V}_t) = 0$ for all t is no longer suboptimal. This means the model can no longer improve and the model output difference between time steps starts to gradually move to zero. We call the epoch for which this first happens the critical epoch e_c . Table (II) gives the average loss for the different models at the final epoch together with e_c .

V. COMPARISON WITH H -FUNCTIONAL

Having fully specified the learning process of the model $h(\mathbf{V}_t)$, let us consider its relation to the H -functional pro-

Layer	Hyperparameter	Activation
Input	Input units: 2	–
Dense	Output units: n_{hidden}	ReLU
Dense	Output units: n_{hidden}	ReLU
Sum pooling	–	–
Dense	Output units: n_{hidden}	ReLU
Dense	Output units: 1	Linear

TABLE I: Model architecture based on the Deepsets [47] architecture described by (10a).

vided in (5). The model $h(\mathbf{V}_t)$ can only possibly resemble the H -functional up to an affine transformation [32, 35]. This is because (11) is invariant under shifts constant in time. Furthermore, we have for $c \in \mathbb{R}$

$$\{h(\mathbf{V}_t), \lambda\} \rightarrow \{ch(\mathbf{V}_t), \lambda/c\} \Rightarrow \mathcal{L}_t^\alpha \rightarrow c\mathcal{L}_t^\alpha , \quad (14)$$

which means we can multiply the function $h(\mathbf{V}_t)$ with a constant factor and it will only affect the loss with a total factor provided we rescale the physically meaningless λ . Therefore, in order to compare the model to the real H -functional we transform the function $h(\mathbf{V}_t)$ as

$$\tilde{h}^{[n]}(\mathbf{V}_t^{[n]}) = a^{[n]}h(\mathbf{V}_t^{[n]}) + b^{[n]} . \quad (15)$$

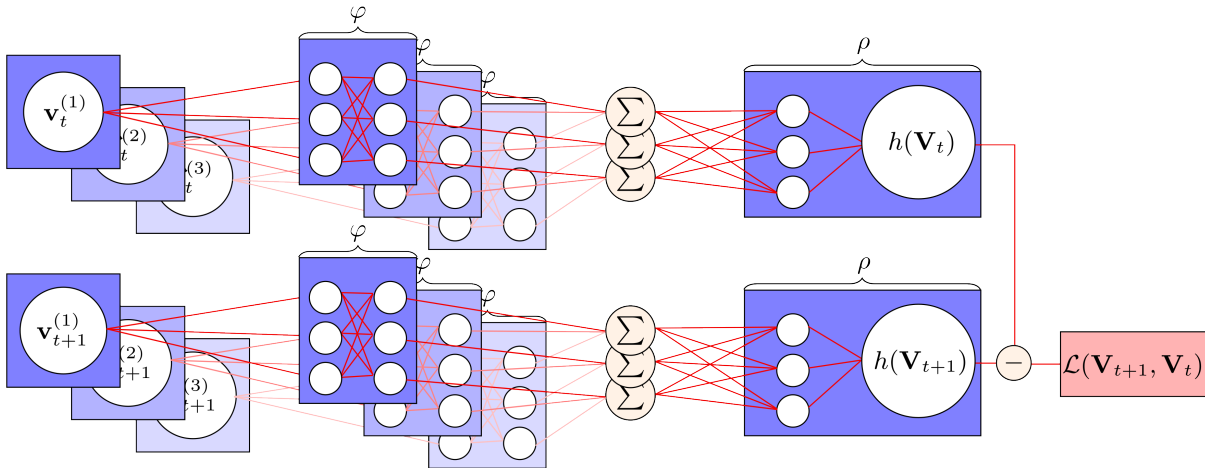


FIG. 4: Schematic picture of the model output combined with that of the next time step to form a loss consistent with a siamese neural network where the inputs of the two time steps are processed with the same model which is of the form of (10a). We considered the case of 3 input vectors $\mathbf{v}_t^{(i)}$ of a single run n whose label we omitted to avoid clutter. For the picture we took $n_{\text{hidden}} = 3$ whereas in reality the n_{hidden} is as in (13).

n_{hidden}	$\langle \mathcal{L}^{\alpha_{\text{final}}}(N_e) \rangle$	$\langle \mathcal{L}^{(0)}(N_e) \rangle$	e_c
16	0.00000950	-0.00001418	95
32	0.00017283	-0.00111001	105
64	0.00003145	-0.00038164	111

TABLE II: Average loss of (11) at final epoch for the different models and the epoch e_c for which $\langle \mathcal{L}^{\alpha(e)} \rangle$ starts to flip sign. We also provided the final loss with $\alpha = 1$ of (10b) as this loss puts the different models on equal footing.

The coefficients $a^{[n]}$ and $b^{[n]}$ are fitted to the H -functional with the least squares algorithm for each separate run n and for all time steps t , i.e. they are computed as

$$\text{argmin}_{a^{[n]}, b^{[n]}} = \sum_t \left(\tilde{h}^{[n]}(\mathbf{v}_t^{[n]}) - H_t^{[n]} \right)^2. \quad (16)$$

In Fig. 5, the result is shown for the different models and compared to the H -functional. It is clear that for $n_{\text{hidden}} = 32$ the model performs better than for $n_{\text{hidden}} = 16$, whereas there is no big difference between $n_{\text{hidden}} = 64$ and $n_{\text{hidden}} = 32$. Although the affine parameters are fitted for each run separately, we would ideally have a model that can provide a value for the H -functional that is consistent throughout all runs. To find out whether the model is consistent throughout runs, we compute the average and the variance of the affine parameters in Table III. We see that going from $n_{\text{hidden}} = 16$ to $n_{\text{hidden}} = 32$ lowers the error, which indicates a better learning process, whereas $n_{\text{hidden}} = 64$ slightly increases it, although the coefficient of variation of the affine parameters is lowered significantly, suggesting that it is a

more coherent model. Note that $\langle a \rangle$ is always negative as the model learns a function that increases in time whereas the H -functional is defined to be decreasing in time as follows from (6a).

n_{hidden}	MSE	$\langle a \rangle$	$\langle b \rangle$	$\text{CV}(a)$	$\text{CV}(b)$
16	0.0429	-448.216	-9452.722	0.0430	0.0433
32	0.0155	-4.622	1104.860	0.0487	0.0462
64	0.0171	-14.885	-380.249	0.0215	0.0221

TABLE III: Mean affine parameters $\langle a \rangle$, $\langle b \rangle$; coefficient of variation $\text{CV}(x) = \sqrt{\text{Var}(x)} / |\langle x \rangle|$; and mean-squared-error loss of the affine fits for the different models.

VI. DISCUSSION

In this work we used a siamese neural network to learn the H -functional of H -theorem for sequential data of a numerical simulation of a thousand hard disks colliding with each other after being initialized in a low-entropy state. The loss function that was formulated in order to learn H -theorem was based on the requirement that the learned function should attribute higher values to input data corresponding to later points in time. This requirement forces the model to identify the arrow of time which according to H -theorem was predicted to exist for this simple but also infinitely chaotic model of hard disks. The resulting model only resembles the extracted H -functional after an appropriately fitted affine transformation. Two things that were found to be important for

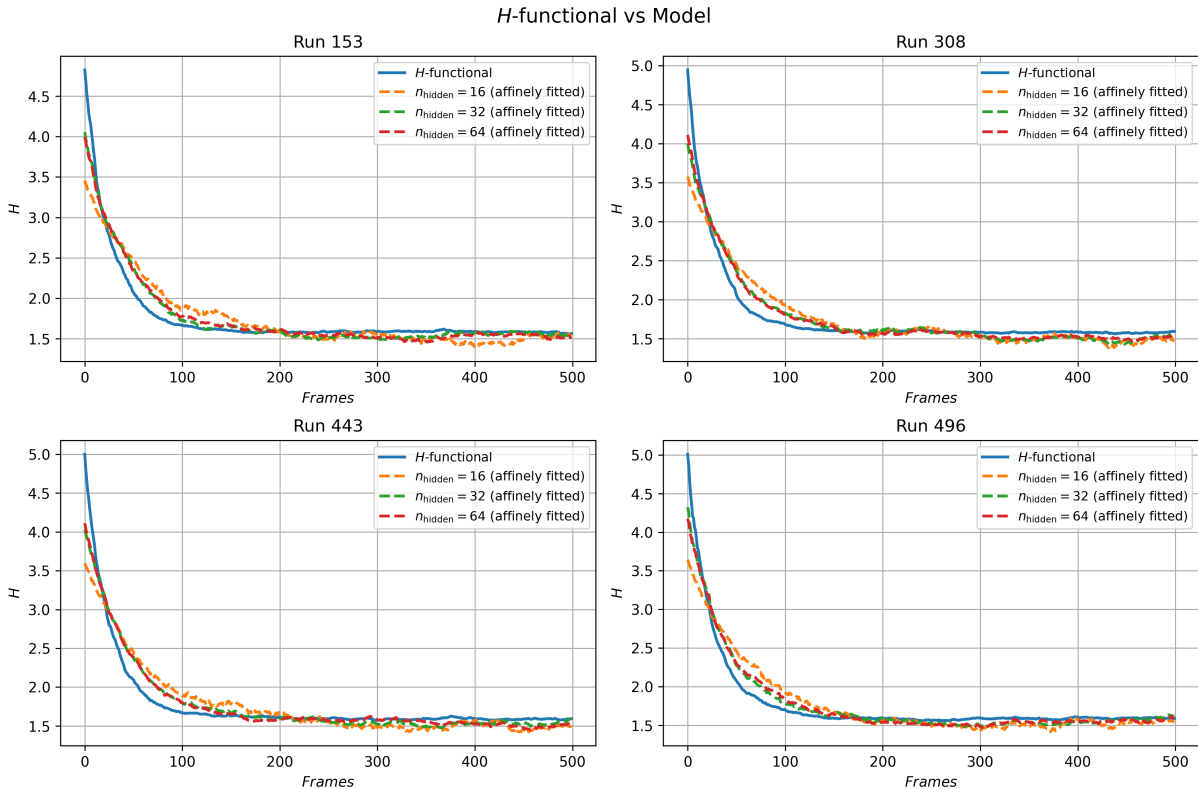


FIG. 5: Picture of H -functional given by (5) vs affinely fitted model output. When computing the H -functional, we used the same bin size that was also used in Fig. 3 to perform a Riemann sum.

making the model resemble the H -functional are

1. The DeepSets architecture [47], which implements the permutation invariance of the particle labels, thereby drastically simplifying the model compared to a model that treats every particle separately.
2. The sign-dependent tilt of the loss which makes it so that at late epochs, the model is penalized more strongly for outputting a decrease in time than it is rewarded for outputting an increase, thereby generating a model that is less oscillatory at late times and steeper at short times.

In future work, it would be interesting to explore more complicated types of collisional interactions, such as for example polyatomic gases [51] or for active gas of two

species of hard spheres that collide reactively and can resemble the phenomenon of bird flocking [28].

VII. METHODS

The training of the PyTorch model was performed on the Snellius supercomputer at SURF, the Dutch national supercomputing facility. The source code developed for this study is openly available at <https://github.com/rubenlier/Machine-Learning-H-theorem>.

VIII. ACKNOWLEDGEMENTS

We thank Roy Stegeman and Karthik Viswanathan for useful discussions.

-
- [1] Ludwig Boltzmann. Weitere studien über das wärmeleichgewicht unter gasmolekülen. *Sitzungsberichte der Akademie der Wissenschaften, Mathematisch-Naturwissenschaftliche Klasse*, 66(3, Zweite Abteilung):275–370, 1872.
 - [2] Ludwig Boltzmann. Zu hrn. zermelo’s abhandlung “über die mechanische erklärungen irreversibler vorgänge”.

- [3] E. Zermelo. Ueber einen satz der dynamik und die mechanische wärmetheorie. *Annalen der Physik*, 293(3):485–494, 1896.
- [4] E. Zermelo. Ueber mechanische Erklärungen irreversibler Vorgänge. Eine Antwort auf Hr. Boltzmann’s “Entgegnung”. *Annalen der Physik*, 295(12):793–801, 1896.

- [5] Cédric Villani. Cercignani’s conjecture is sometimes true and always almost true. *Communications in Mathematical Physics*, 234(3):455–490, Mar 2003.
- [6] Thomas Borsoni. Extending cercignani’s conjecture results from boltzmann to boltzmann–fermi–dirac equation. *Journal of Statistical Physics*, 191(5):52, Apr 2024.
- [7] R. Alexandre and C. Villani. On the boltzmann equation for long-range interactions. *Communications on Pure and Applied Mathematics*, 55(1):30–70, 2002.
- [8] R. J. DiPerna and P. L. Lions. On the cauchy problem for boltzmann equations: Global existence and weak stability. *The Annals of Mathematics*, 130(2):321, September 1989.
- [9] Carlo Cercignani. *Ludwig Boltzmann: the man who trusted atoms*. Oxford University Press, London, England, January 2006.
- [10] Carlo Cercignani. *The Boltzmann Equation and Its Applications*. Springer New York, 1988.
- [11] Arthur Stanley Eddington. *The Nature of the Physical World*. Cambridge University Press, Cambridge, England, 1st edition, 1929.
- [12] Richard C. Tolman. The principle of microscopic reversibility. *Proceedings of the National Academy of Sciences*, 11(7):436–439, 1925.
- [13] Harold Grad. On the kinetic theory of rarefied gases. *Communications on Pure and Applied Mathematics*, 2(4):331–407, 1949.
- [14] M. Born and H. S. Green. A general kinetic theory of liquids. i. the molecular distribution functions. *Proceedings of the Royal Society of London. Series A, Mathematical and Physical Sciences*, 188(1012):10–18, 1946.
- [15] Oscar E. Lanford. Time evolution of large classical systems. In Jürgen Moser, editor, *Dynamical Systems, Theory and Applications*, pages 1–111. Springer, Berlin, Heidelberg, 1975.
- [16] Oscar E. Lanford III. On a derivation of the Boltzmann equation. In *International conference on dynamical systems in mathematical physics*, number 40 in *Astérisque*, pages 117–137. Société mathématique de France, 1976.
- [17] Herbert Spohn. Kinetic equations from hamiltonian dynamics: Markovian limits. *Rev. Mod. Phys.*, 52:569–615, Jul 1980.
- [18] S. Chapman and T.G. Cowling. *The Mathematical Theory of Non-uniform Gases: An Account of the Kinetic Theory of Viscosity, Thermal Conduction and Diffusion in Gases*. Cambridge Mathematical Library. Cambridge University Press, 1990.
- [19] Andrew Lucas and Sean A. Hartnoll. Kinetic theory of transport for inhomogeneous electron fluids. *Phys. Rev. B*, 97:045105, Jan 2018.
- [20] Markus Mueller, Joerg Schmalian, and Lars Fritz. Graphene - a nearly perfect fluid, 2009.
- [21] Inti Sodemann and Liang Fu. Quantum nonlinear hall effect induced by berry curvature dipole in time-reversal invariant materials. *Phys. Rev. Lett.*, 115:216806, Nov 2015.
- [22] S R De Groot and etc. *Relativistic kinetic theory*. Elsevier Science, London, England, October 1980.
- [23] Carlo Cercignani and Gilberto M Kremer. *The relativistic Boltzmann equation: Theory and applications*. Progress in Mathematical Physics. Birkhauser Verlag AG, Basel, Switzerland, 2002 edition, February 2002.
- [24] A.H. Mueller and D.T. Son. On the equivalence between the boltzmann equation and classical field theory at large occupation numbers. *Physics Letters B*, 582(3–4):279–287, March 2004.
- [25] Thomas Ihle. Kinetic theory of flocking: Derivation of hydrodynamic equations. *Phys. Rev. E*, 83:030901, Mar 2011.
- [26] Eric Bertin, Michel Droz, and Guillaume Grégoire. Boltzmann and hydrodynamic description for self-propelled particles. *Phys. Rev. E*, 74:022101, Aug 2006.
- [27] Kevin T. Grosvenor, Niels A. Obers, and Subodh P. Patil. Hydrodynamics without boost-invariance from kinetic theory: From perfect fluids to active flocks, 2025.
- [28] Ruben Lier. A microscopically reversible kinetic theory of flocking. arXiv:2508.09274 [cond-mat], 2025.
- [29] Alireza Seif, Mohammad Hafezi, and Christopher Jarzynski. Machine learning the thermodynamic arrow of time. *Nature Physics*, 17(1):105–113, Jan 2021.
- [30] Gavin E. Crooks. Entropy production fluctuation theorem and the nonequilibrium work relation for free energy differences. *Phys. Rev. E*, 60:2721–2726, Sep 1999.
- [31] C. Jarzynski. Nonequilibrium equality for free energy differences. *Phys. Rev. Lett.*, 78:2690–2693, Apr 1997.
- [32] Hiroto Kuroyanagi and Tatsuro Yuge. Deep learning of thermodynamic laws from microscopic dynamics, 2025.
- [33] Elliott H. Lieb and Jakob Yngvason. The physics and mathematics of the second law of thermodynamics. *Physics Reports*, 310(1):1–96, 1999.
- [34] Donglai Wei, Joseph J. Lim, Andrew Zisserman, and William T. Freeman. Learning and using the Arrow of time. In *Proceedings of the IEEE Conference on Computer Vision and Pattern Recognition (CVPR)*, June 2018.
- [35] Nasim Rahaman, Steffen Wolf, Anirudh Goyal, Roman Remme, and Yoshua Bengio. Learning the Arrow of time, 2019.
- [36] Teodor Mihai Moldovan and Pieter Abbeel. Safe exploration in markov decision processes, 2012.
- [37] Alexander Hans, Daniel Schneegass, Anton Schäfer, and Steffen Udluft. Safe exploration for reinforcement learning, 01 2008.
- [38] B. J. Alder and T. E. Wainwright. Decay of the velocity autocorrelation function. *Phys. Rev. A*, 1:18–21, Jan 1970.
- [39] Alessandro Taloni, Yasmine Meroz, and Adrián Huerta. Collisional statistics and dynamics of two-dimensional hard-disk systems: From fluid to solid. *Phys. Rev. E*, 92:022131, Aug 2015.
- [40] B. J. Alder and T. E. Wainwright. Velocity autocorrelations for hard spheres. *Phys. Rev. Lett.*, 18:988–990, Jun 1967.
- [41] J. Orban and A. Bellemans. Velocity-inversion and irreversibility in a dilute gas of hard disks. *Physics Letters A*, 24(11):620–621, 1967.
- [42] Harold Grad. Principles of the kinetic theory of gases. In Siegfried Flüge, editor, *Handbuch der Physik, Band 12: Thermodynamik der Gase*, pages 205–294. Springer-Verlag, Berlin, Göttingen, Heidelberg, 1958.
- [43] Clément Mouhot and Lorenzo Pareschi. Fast algorithms for computing the Boltzmann collision operator. *Mathematics of Computation*, 75(256):1833–1852, July 2006.
- [44] Tianbai Xiao and Martin Frank. Using neural networks to accelerate the solution of the Boltzmann equation.

- Journal of Computational Physics, 443:110521, October 2021.
- [45] Tianbai Xiao and Martin Frank. Relaxnet: A structure-preserving neural network to approximate the Boltzmann collision operator. Journal of Computational Physics, 490:112317, October 2023.
- [46] Christian Hill. The Maxwell–Boltzmann distribution in two dimensions. <https://scipython.com/blog/the-maxwellboltzmann-distribution-in-two-dimensions/>, July 2020. Learning Scientific Programming with Python.
- [47] Manzil Zaheer, Satwik Kottur, Siamak Ravanbakhsh, Barnabás Póczos, Ruslan Salakhutdinov, and Alexander J Smola. Deep sets. In Proceedings of the 31st International Conference on Neural Information Processing Systems, NIPS’17, page 3394–3404, Red Hook, NY, USA, 2017. Curran Associates Inc.
- [48] Jane Bromley, Isabelle Guyon, Yann LeCun, Eduard Säckinger, and Roopak Shah. Signature verification using a “siamese” time delay neural network. In Advances in Neural Information Processing Systems, volume 6, pages 737–744. Morgan-Kaufmann, 1993.
- [49] Chris Burges, Tal Shaked, Erin Renshaw, Ari Lazier, Matt Deeds, Nicole Hamilton, and Greg Hullender. Learning to rank using gradient descent. In Proceedings of the 22nd International Conference on Machine Learning, ICML ’05, page 89–96, New York, NY, USA, 2005. Association for Computing Machinery.
- [50] Diederik P. Kingma and Jimmy Ba. Adam: A method for stochastic optimization, 2017.
- [51] Carlo Cercignani and Maria Lampis. On the h-theorem for polyatomic gases. Journal of Statistical Physics, 26(4):795–801, December 1981.